

## HIGH-POWER MODULAR INVERTER DEVELOPMENT FOR ELECTRIC MOTOR TESTING PURPOSES

ZOLTÁN SZELI\*<sup>1</sup> AND GÁBOR SZAKÁLLAS<sup>1</sup>

<sup>1</sup>Research Center of Vehicle Industry, Széchenyi István University, Egyetem tér 1, Győr, 9026, HUNGARY

This paper presents the development process of a high-power modular inverter system. The goal was to develop a universal inverter system (motor controller + power electronics) in which the performance of the power stage is scalable. The design concepts, hardware architecture, system components, built-in features and protections are described regarding the power stage.

**Keywords:** modular, universal, desaturation, active clamping, protection

### 1. Introduction

Power electronics and their control algorithms are very important parts of electric vehicles. The whole system can operate reliably, efficiently and with good dynamics only if all elements of the vehicle are well coordinated. Before the different electric drivetrains can finally be applied, they should be tested under different circumstances on electric motor or drivetrain test benches. Otherwise it would be difficult to test them in-vehicle as they are already built-in. For such testing processes, a flexible test system is a good solution that can be easily modified at both hardware and software levels, especially for institutions like our research center where various types of electric motors from different manufacturers are dealt with. Their inverter systems are usually inaccessible without the help of experts.

### 2. Design Concept

The purpose of the development was to design a universal and scalable (at the power stage) inverter system. Thus, the same system can be used for three-phase electrical machines with different power requirements and applications. The first version is capable of 600 A at a nominal system voltage of 400 V. As the motor controller is equipped with standard interfaces, it is able to adapt power stages to different power levels. For the design of the hardware for the motor controller and power stage, state-of-the-art solutions were used.

Furthermore, different motor control algorithms are dealt with at the research center, so it was decided to use them with the motor controller to ensure the software en-

vironment is capable of further developments and different types of motors can be easily adapted to it. Motor control software can be implemented using model-based simulation (MATLAB/Simulink) with automatic code generation. As a result, the behaviour of the motor can be determined in advance by simulation and easily adapted to our specific environment.

The system supports different communication protocols, e.g. CAN, RS232, Ethernet and FlexRay, which can be used for control, data acquisition and status information polling. The system is usually used to test three-phase electric machines or can be installed in electric vehicles.

### 3. Results and Analysis

The inverter system (Fig. 1) consists of four separate printed circuit boards (PCBs), namely Control Board,

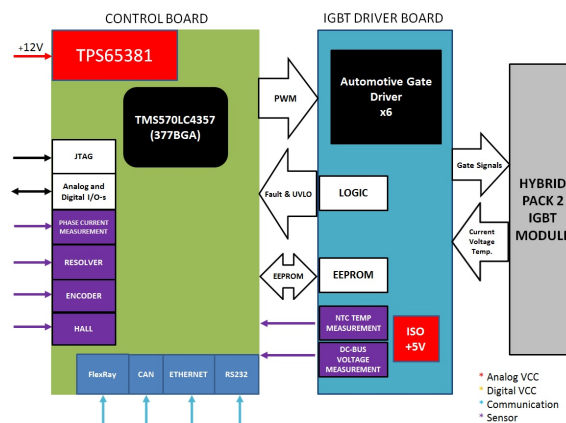


Figure 1: Hardware structure

\*Correspondence: szgabor@ga.sze.hu

Power Stage, F-S-800 Insulated Gate Bipolar Transistor (IGBT) Interface Board, and a Current Measurement Board for current transducers. Only commercially available and automotive qualified components were used for the hardware. With regard to the different circuits on the boards, the SPICE simulator was used to support the design.

The main features:

- Undervoltage protection
- Overcurrent protection
- Isolated sensor supply
- Isolated voltage measurement
- Isolated DC/DC power supply for the IGBT drivers
- Temperature measurements
- Built-in protections:
  - Surge protector
  - Short circuit
  - Desaturation
  - Advanced Active Clamping

### 3.1 Power stage

The power stage was designed to be able to drive a maximum of two IGBT modules simultaneously (one IGBT module can also be used by us). Thus, the output power of the inverter is scalable and can easily be doubled should a different IGBT module be used.

### 3.2 Isolated power supply for the gate drivers

The power stage includes 6 separate Flyback DC/DC converters that produce an isolated +15 V / -8 V asymmetrical power supply for IGBT gate drivers as seen in Fig. 2.

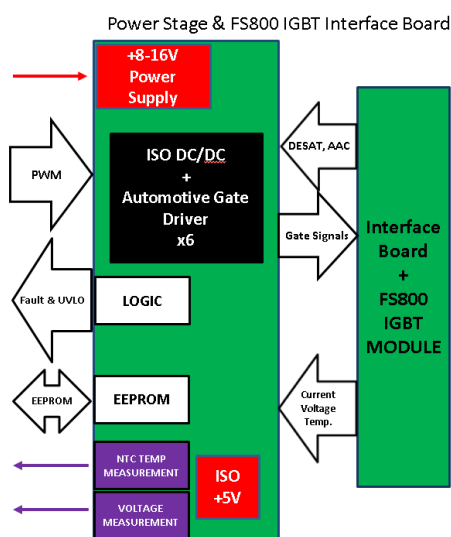


Figure 2: Power stage

Design parameters according to the system requirements and the Flyback Converter datasheet [1]:

- 8-18 V DC input voltage
- -8 V / +15 V output voltage
- 10 W output power (due to IGBTs in parallel,  $f_{sw} = 20$  kHz)
- 3, 956 W power consumption per IGBT module was calculated from [2]

$$P_{Gdr} = Q_G (V_{GE(on)} - V_{GE(off)}) f_{sw} \quad (1)$$

The output power selected was chosen for 2 IGBT modules in parallel.

The isolated power supply for the gate drivers works as expected in the real circuit, as can be seen in Figs. 3 and 4.

### 3.3 Gate drive circuit

The IGBT modules were powered by Infineon's 1ED020I12FA2 galvanically isolated single channel IGBT gate driver circuits, which were placed on a separate PCB. The maximum output current of the 1ED020I12FA2 driver was  $\pm 2$  A. Because of this low peak current, significantly increased gate resistors were required, which greatly degraded the switching properties of the IGBT driver. Therefore, it was necessary to

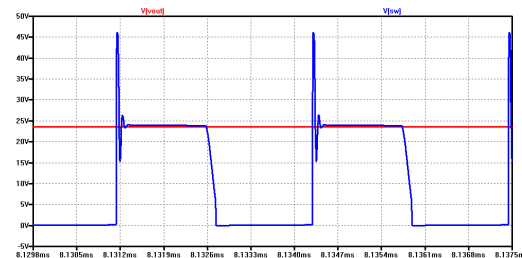


Figure 3: Simulated Flyback DC/DC switching waveform ( $P_{out} = 5$  W)

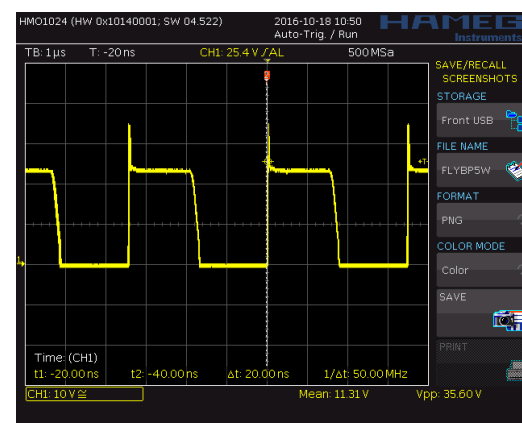


Figure 4: Flyback DC/DC switching oscilloscope waveform ( $P_{out} = 5$  W)

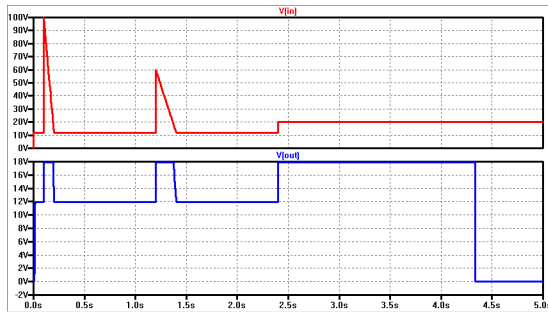


Figure 5: Operation of the surge stopper protection

use a so-called Bipolar Totem-Pole amplifier between the output of the driver and the IGBT gate terminal. The designed Bipolar Totem-Pole circuit was capable of driving the IGBT with the use of a resistor of  $R_{Goff} = 0.82 \Omega$ .

### 3.4 Built-in features

**Surge stopper** The voltage supply (+8 V – +16 V) was connected to the load through an overvoltage protection circuit. This circuit protects the other parts of the power stage from high voltage spikes and controls the output voltage in case of input overvoltages (Load Dumps) as shown in Fig. 5. It is also equipped with over-current and reverse polarity protection as well as an adjustable low-voltage fault detection limit.

**Desaturation protection** The IGBT driver is a power semiconductor that is normally used to switch operation in the closed and saturation regions. The closed region can be considered to be a broken wire, and in the saturation region it functions as a short circuit. Between the IGBT collector and emitter terminals, the saturation voltage,  $V_{CE}$ , can be measured [3]. This voltage depends on the temperature of the semiconductor, its collector current and the voltage applied to the gate. Fig. 6 shows the dependence of the saturation voltage of the FS800R07A2E3

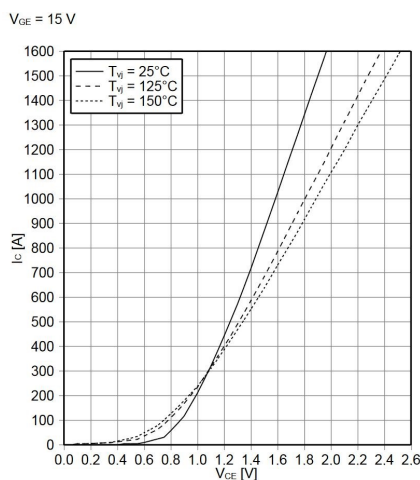


Figure 6: Output characteristics of the FS800R07A2E3 IGBT module

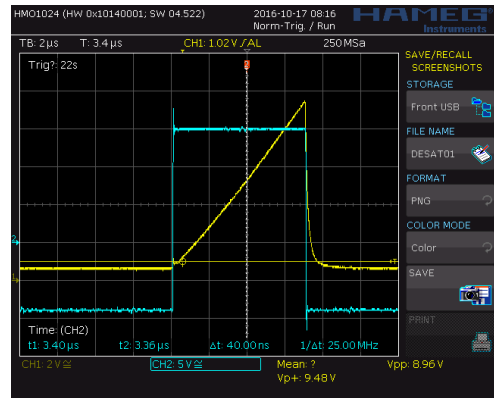


Figure 7: Operation of the desaturation protection

IGBT module with regard to its collector current on the temperature of the semiconductor.

The desaturation voltage can be adjusted using Zener or fast diodes, so in our case, the threshold voltage,  $V_{CE}$ , selected of 1.3 V used in the switching will be subject to a 600 A collector current limitation per module at 25 °C.

The IGBT driver circuit is continuously monitoring the  $V_{CE}$ , using a comparator, and if that exceeds the reference voltage, that is 9 V, of the integrated circuit, the driver forces its output to VEE2 (–8 V) within a maximum  $T_{DESATOUT}$  time of 430 ns as shown in Fig. 7. With this kind of protection, short-circuit failures can be avoided and a temperature-dependent current limitation realized. The  $V_{CE}$  can be monitored only after a period of time equal to  $T_{BLANKING} + T_{DESATOUT}$  ( $1.8 \mu s + 430 \text{ ns} = 2.23 \mu s$ ) has elapsed following the arrival of the control signal [4].

The fault signal is only active when the IGBT driver is switched on.

**Advanced Active Clamping** When working with IGBTs, parasitic inductances inside them and the converter circuits must be taken into consideration. Their effects cannot be completely eliminated for physical reasons and their influence on the system behaviour cannot be neglected. Fig. 8 shows the parasitic inductances contained in a commutation circuit.

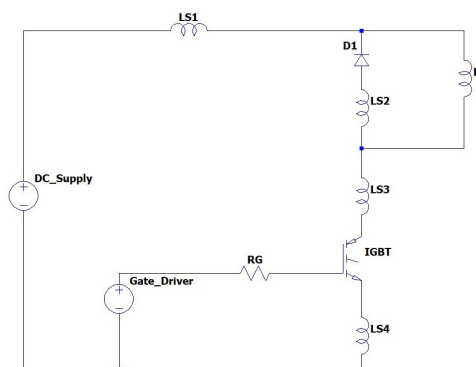


Figure 8: Parasitic inductances in IGBTs

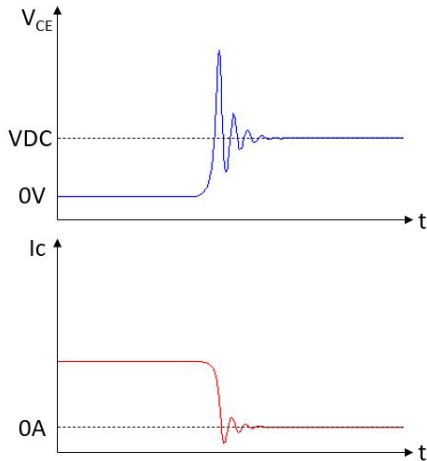


Figure 9: Characteristics of the IGBT turn-off process

Voltage transients are produced at the collector of the IGBTs during their turn-off process, which are caused by the change in current passing through them as shown in Fig. 9. The commutation speed and thus, the turn-off overvoltage at an IGBT can, in principle, be affected by the turn-off gate resistance  $R_{Goff}$ . This technique is used most often in low-power devices where  $R_{Goff}$  must be selected for overload conditions such as turn-off of the double rated current, short circuits and a temporarily increased link circuit voltage. During normal operations, this causes increased turn-off switching losses and turn-off delays, which reduce the efficiency of the modules [5].

The FS800R07A2E3 IGBT module has a parasitic inductance of 14 nH.

To reduce the voltage spikes, a clamping circuit was used that allows charging of the gate-emitter capacitance and flow charges to the base of the proposed Bipolar Totem-Pole over the specified voltage range through a transient-voltage-suppression diode connected between the collector and the gate, driving the IGBT into the normal active mode and reducing the current-change rate,  $dI_C/dt$  as seen in Figs. 10 and 11.

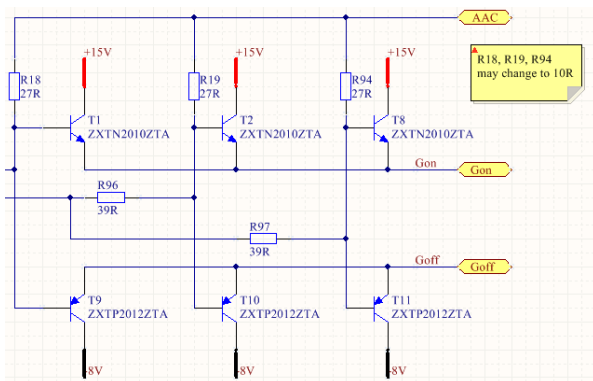


Figure 10: The proposed Bipolar Totem-Pole layout with feedback

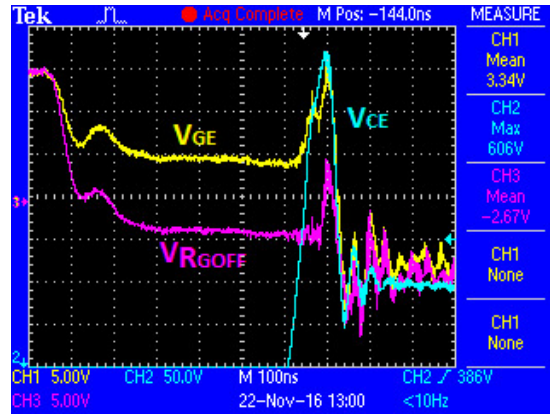


Figure 11: Operation of the Advanced Active Clamping circuit @ 340 V/ 800 A (single IGBT module)

This type of control of the Bipolar Totem-Pole circuit reduces the power dissipation as a result of the resistance  $R_{Goff}$  whilst operating.

### 3.5 Cooling system

To design the cooling system of the inverter, thermal simulations were carried out. The maximum power dissipation of the IGBT module was 1500 W, and its operating temperature range was between  $-40$  and  $150$  °C. The thermal resistance between the liquid coolant (50% water, 50% glycol) and the surface of the heatsink was 0.097 K/W.

The IGBT manufacturing drawings were used to design the 3D model as seen in Fig. 12.

## 4. Conclusion

The functional testing of an inverter was carried out at the Electric Motor Test Bench Laboratory of Széchenyi István University. The developed system and the test environment can be seen in Figs. 13 and 14. A permanent-magnet synchronous motor (PMSM) was connected to it and different peripherals and built-in functions tested. On the other side of the test bench, the same type of PMSM connected to a 400 V / 500 A, downscaled (single IGBT module) version of the inverter was used. At first, the tests were performed at a speed of 1600 rpm and at low load

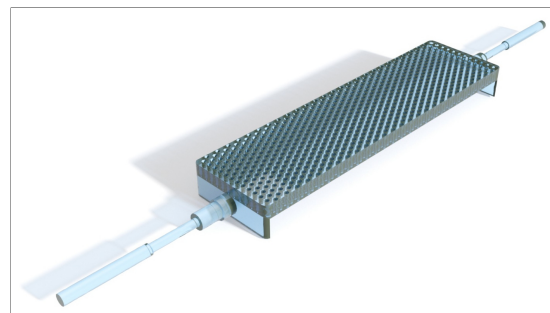


Figure 12: The designed coolant space inside the heatsink

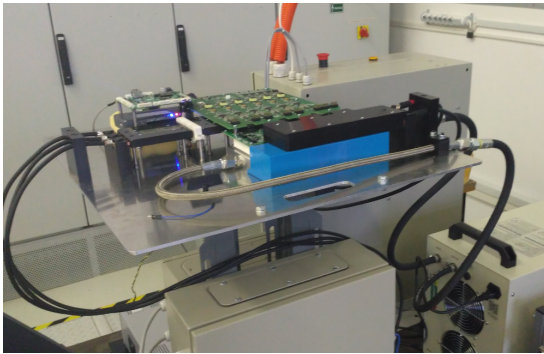


Figure 13: The assembled inverter system

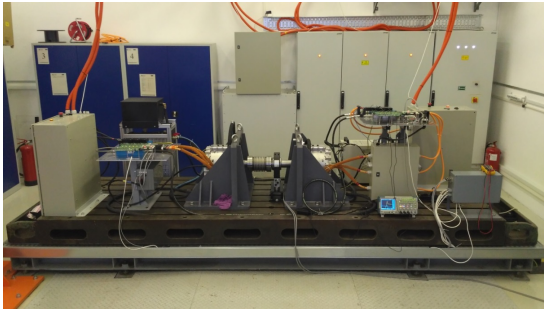


Figure 14: Electric motor test bench with the mounted inverters

torques. The inverters were operated alternately, one in torque-control mode, the other in speed-control mode. In a future paper, these inverters will be tested under heavy-

load conditions, when the motor control algorithms work reliably.

## Acknowledgements

The research was carried out as part of the "Autonomous Vehicle Systems Research related to the Autonomous Vehicle Proving Ground of Zalaegerszeg (EFOP-3.6.2-16-2017-00002)" project in the framework of the New Széchenyi Plan. The completion of this project is funded by the European Union and co-financed by the European Social Fund.

## REFERENCES

- [1] Linear Technology, "Flyback, Forward and Isolated Controllers", LT8302 Datasheet, Sept. 2016 Rev. C
- [2] Infineon Technologies AG, "Automotive IGBT Module Explanation of Technical Information", Application Note AN2010-09, 2010
- [3] Avago Technologies, "Desaturation Fault Detection", Application Note AN5324, 2012
- [4] Infineon Technologies AG, "Galvanic Isolated Gate Driver", 1ED020I12FA2 Datasheet, May 2013 Rev. 2.0
- [5] Rüedi, H.; Thalheim, J.; Garcia, O.: Advantages of Advanced Active Clamping, *Power Electronics Europe*, 2009 **8**, 27–29